INTERNATIONAL JOURNAL FOR NUMERICAL METHODS IN FLUIDS
Int. J. Numer. Meth. Fluids 2005; **48**:91–97
Published online 3 March 2005 in Wiley InterScience (www.interscience.wiley.com). DOI: 10.1002/fld.944

Numerical solution of single and multi-phase internal transonic flow problems[‡]

J. Dobeš[*,†], J. Fořt and J. Halama

Department of Technical Mathematics, Faculty of Mechanical Engineering, Czech Technical University, Karlovo Nám. 13, CZ-121 35 Prague, Czech Republic

SUMMARY

This paper presents numerical methods for solving turbulent and two-phase transonic flow problems. The Navier–Stokes equations are solved using cell-vertex Lax–Wendroff method with artificial dissipation or cell-centred upwind method with Roe's Riemann solver and linear reconstruction. Due to a big difference of time scales in two-phase flow of condensing steam a fractional step method is used. Test cases including 2D condensing flow in a nozzle and one-phase transonic flow in a turbine cascade with transition to turbulence are presented. Copyright © 2005 John Wiley & Sons, Ltd.

KEY WORDS: finite volume method; fractional step method; condensation; transonic flow; turbine cascades

1. INTRODUCTION

Condensation of steam appears e.g. in last stages of large enterprise turbines, where it decreases machine efficiency and durability of the blades. A flow model, which can describe such a flow including condensation and turbulence phenomena is presented [1]. Turbulence transition is also considered.

2. GOVERNING EQUATIONS

Two-phase flow in this paper means the flow of the mixture of vapour and water droplets. We consider following simplifications: condensation is homogenous; droplets are convected

[*]Correspondence to: Jiří Dobeš, Department of Technical Mathematics, Faculty of Mechanical Engineering, Czech Technical University, Karlovo Nám. 13, CZ-121 35 Prague, Czech Republic.
[†]E-mail: dobes@marian.fsik.cvut.cz
[‡]This was originally submitted as part of the ICFD SPECIAL ISSUE.

Contract/grant sponsor: Grant Agency of the Czech Republic; contract/grant number: 201/05/0005
Contract/grant sponsor: Research plan of MSMT; contract/grant number: 6840770003

Received 27 April 2004
Revised 13 January 2005
Accepted 13 January 2005

by the vapour; the wetness (mass fraction of droplets) is small i.e. volume of droplets can be neglected; the pressure of the mixture is approximated by the pressure of vapour; droplets are described by the Hill's approximation [2].

Condensation has two different mechanisms, nucleation (creation of new droplets) and droplet growth. Nucleation starts, when the vapour temperature drops sufficiently below the saturation temperature (typically between 30 and 40 K). The size of new droplets is given by the value of critical radius. The number of new droplets is given by the nucleation rate J according to Becker and Döring [3], which gives the number of new droplets per unit volume. The growth of existing droplet depends on the temperature of surrounding vapour. We use the relation of Valha [4] for time derivative of droplet radius $\dot{r}$. Material properties of vapour are taken from the steam tables in the form of polynomial functions of temperature and pressure. For the modeling of the droplets we have chosen Hill's approximation. Whole droplet size spectrum is approximated by parameters

$$Q_0 = n, \quad Q_1 = \sum_{i=1}^{n} r_i, \quad Q_2 = \sum_{i=1}^{n} r_i^2, \quad r = \sqrt{Q_2/Q_0} \tag{1}$$

where n denotes the total number of droplets per unit mass of the mixture, r_i is the radius of ith droplet and r is the average radius.

The Navier–Stokes equations for the 2D flow of the mixture[‡] and the conservation equations for variables Q_0, Q_1, Q_2 can be written together as a one system of partial differential equations in conservative form (2)

$$\frac{\partial}{\partial t}\mathbf{W} = -\frac{\partial}{\partial x}\mathbf{F}^c + \frac{\partial}{\partial x}\mathbf{F}^v - \frac{\partial}{\partial y}\mathbf{G}^c + \frac{\partial}{\partial y}\mathbf{G}^v + \mathbf{P} \tag{2}$$

$$\mathbf{W} = [\rho, \rho u_x, \rho u_y, e, \rho w, \rho w Q_2, \rho w Q_1, \rho w Q_0]^{\mathrm{T}}$$

$$\mathbf{F}^c = [\rho u_x, \rho u_x^2 + p, \rho u_x u_y, (e+p)u_x, \rho w u_x, \rho w Q_2 u_x, \rho w Q_1 u_x, \rho w Q_0 u_x]^{\mathrm{T}}$$

$$\mathbf{F}^v = [0, \tau_{xx}, \tau_{xy}, u_x\tau_{xx} + u_y\tau_{xy} - q_x, 0, 0, 0, 0]^{\mathrm{T}}$$

$$\mathbf{G}^c = [\rho u_x, \rho u_y u_x, \rho u_y^2 + p, (e+p)u_y, \rho w u_y \rho w Q_2 u_y, \rho w Q_1 u_y, \rho w Q_0 u_y]^{\mathrm{T}}$$

$$\mathbf{G}^v = [0, \tau_{xy}, \tau_{yy}, u_x\tau_{xy} + u_y\tau_{yy} - q_y, 0, 0, 0, 0]^{\mathrm{T}}$$

$$\mathbf{P} = \left[0, 0, 0, 0, \rho\left(\frac{4}{3}\pi r_c^3 \rho_l \frac{J}{\rho} + \frac{4}{3}\pi 3 Q_2 \dot{r} \rho_l\right), \rho\left(r_c^2 \frac{J}{\rho} + 2Q_1\dot{r}\right), \rho\left(r_c \frac{J}{\rho} + Q_0\dot{r}\right), \rho\ \frac{J}{\rho}\right]^{\mathrm{T}}$$

where the first four equation are the Navier–Stokes equation for the mixture and the last four equations are the transport equations for mass of droplets, Q_2, Q_1 and Q_0, respectively. The symbol ρ denotes mixture density, u_x and u_y mixture velocity components, p pressure, e total energy of mixture per unit volume, w wetness, ρ_l denotes the density of liquid phase, r_c denotes the critical radius, τ_{xx}, τ_{xy}, τ_{yy} are shear stresses given by Newton law, q_x, q_y are

[‡]The droplets are of course 3D phenomenon. The 2D model is considered in a sense of 3D flow uniform in the z-direction and with zero z-component of velocity. The Hill's model then can be used also in 2D.

heat fluxes given by Fourier law, t time and x and y spatial coordinates. The first four and the last four equations are coupled by the equation for the pressure according to Šťastný [5]

$$p = (\gamma - 1)\frac{(1-w)}{1+w(\gamma-1)}\left[e - \frac{1}{2}\rho(u_x^2 + u_y^2) + \rho w L\right] \tag{3}$$

where γ is the specific heat ratio considered as a function of temperature $\gamma = c_p(T)/(c_p(T) - R_v)$. Condensation is taken into account only for inviscid or laminar flow model (above equations). One-phase flow model (RANS) is considered in the case of turbulent flow. For encountering of turbulence effects we use models based on a turbulent viscosity, namely modification of algebraic model of Baldwin and Lomax and one equation model of Spalart and Allmaras. We can specify transition onset and offset by intermittency coefficient varying from zero in laminar flow to one in fully turbulent flow. Point of transition is computed using integral boundary layer method.

2.1. Formulation of the problem

Integral form of Equation (2) is solved in the computational domain. For the inlet we prescribe total speed of sound a_0, total density ρ_0 and velocity angle α. For the outlet we prescribe integral value of static pressure p. On the wall we prescribe no-slip condition and condition of adiabatic wall. Point-to-point periodic boundary condition is also considered. The system of conditions is completed by suitable Neumann's conditions. Jacobian of the transport equations has only one multiple eigenvalue u, hence only entering characteristic is in the inlet boundary, where we prescribe dry steam conditions ($w = Q_i = 0$). Value of turbulent viscosity for the Spalart–Allmaras turbulence model is set to zero at the inlet and along the wall and the normal derivative of the turbulent viscosity is prescribed zero at the inlet and the outlet.

3. NUMERICAL METHODS

We use cell-vertex and cell-centred methods. The cell-vertex finite volume method is based on the Lax–Wendroff scheme, i.e. the value of $\mathbf{W}_{i,j}^{n+1}$ is calculated from following Taylor expansion

$$\mathbf{W}_{i,j}^{n+1} = \mathbf{W}_{i,j}^{n} + \Delta t \left.\frac{\partial \mathbf{W}}{\partial t}\right|_{i,j}^{n} + \frac{\Delta t^2}{2}\left.\frac{\partial^2 \mathbf{W}}{\partial t^2}\right|_{i,j}^{n} \tag{4}$$

where the first order term is evaluated on the finite volume $V_{i,j}$ and the second order terms is evaluated on dual finite volume $V_{i,j}^*$, see Figure 1. The second time derivative is treated in

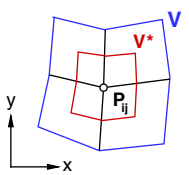

Figure 1. Finite volumes for cell-vertex method.

the following way:

$$\frac{\partial}{\partial t}\left(\frac{\partial \mathbf{W}}{\partial t}\right)=-\frac{\partial}{\partial t}\left(\frac{\partial \mathbf{F}}{\partial x}+\frac{\partial \mathbf{G}}{\partial y}-\frac{\partial \mathbf{P}}{\partial t}\right)=-\frac{\partial}{\partial x}\left(\frac{\partial \mathbf{F}}{\partial t}\right)-\frac{\partial}{\partial y}\left(\frac{\partial \mathbf{G}}{\partial t}\right)+\frac{\partial \mathbf{P}}{\partial t} \tag{5}$$

remaining time derivatives of vectors **F**, **G** and **P** are calculated numerically

$$\mathbf{W}_{i,j}^{n+1/2}=\mathbf{W}_{i,j}^{n}-\frac{\Delta t}{\mu(V_{i,j})}\oint_{\partial V_{i,j}}(\mathbf{F}^{(1)}(\mathbf{W}^{n}),\mathbf{G}^{(1)}(\mathbf{W}^{n}))\cdot \boldsymbol{n}_{\partial V}\,\mathrm{d}S+\frac{\Delta t}{\mu(V_{i,j})}\iint_{V_{i,j}}\mathbf{P}(\mathbf{W}^{n})\,\mathrm{d}V \tag{6}$$

$$\begin{aligned}\mathbf{W}_{i,j}^{n+1}=\mathbf{W}_{i,j}^{n+1/2}&+\frac{\Delta t^{2}}{2\mu(V_{i,j}^{*})}\iint_{V_{i,j}^{*}}\frac{\mathbf{P}(\mathbf{W}^{n+1/2})-\mathbf{P}(\mathbf{W}^{n})}{\Delta t}\,\mathrm{d}V^{*}\\&-\frac{\Delta t^{2}}{2\mu(V_{i,j}^{*})}\cdot\oint_{\partial V_{i,j}^{*}}\left(\frac{\mathbf{F}^{(0)}(\mathbf{W}^{n+1/2})-\mathbf{F}^{(0)}(\mathbf{W}^{n})}{\Delta t},\frac{\mathbf{G}^{(0)}(\mathbf{W}^{n+1/2})-\mathbf{G}^{(0)}(\mathbf{W}^{n})}{\Delta t}\right)\cdot\boldsymbol{n}_{\partial V}\,\mathrm{d}S^{*}+\mathscr{DISS}_{i,j}^{n}\end{aligned} \tag{7}$$

where $\mathbf{F}^{(\xi)}=\mathbf{F}^{c}-\xi\mathbf{F}^{v}$, $\mathbf{G}^{(\xi)}=\mathbf{G}^{c}-\xi\mathbf{G}^{v}$, $\xi\in\{0;1\}$ and $\boldsymbol{n}_{\partial V}$ denotes the unit vector normal to the boundary of V. The term $\mathscr{DISS}$ is an Jameson type conservative artificial viscosity. The derivatives of velocity and the temperature for viscous fluxes are evaluated using Gauss theorem on finite volumes V.

As the second choice we present cell-centred finite volume method with Roe's Riemann solver with entropy correction, linear reconstruction, Van Leer's or Barth's limiter and explicit Runge–Kutta or implicit Euler backward time stepping. Implicit Euler method for solution in element i can be written as

$$\mathbf{W}_{i}^{n+1}=\mathbf{W}_{i}^{n}-k\mathbf{R}_{i}^{n+1}\approx\mathbf{W}_{i}^{n}-k\left(\mathbf{R}_{i}^{n}+\frac{\partial \mathbf{R}_{i}}{\partial \mathbf{W}}(\mathbf{W}_{i}^{n+1}-\mathbf{W}_{i}^{n})\right) \tag{8}$$

where $\mathbf{R}^{n}$ is an update residual from time level n and k is an constant including time-step. This leads to large system of equation for unknown $\mathbf{W}^{n+1}-\mathbf{W}^{n}$. The system is solved using GMRES method with ILU(0) preconditioning. We evaluate Jacobian matrix numerically using one-sided differences with fixed $\varepsilon=10^{-6}$.

For the one equation turbulence model additional equation has to be solved. We use first order cell centred upwind method. Time integration is explicit or implicit. For the implicit time integration we again use first order Euler time integration, but Jacobian matrix is computed analytically. Positive source terms are treated explicitly, while negative are considered in the computed time level. It enhances stability and robustness of the method.

The time step Δt, which is suitable for the modeling of convection–diffusion part is too big for the modeling of condensation. Therefore we use kind of symmetric fractional step method

$$\frac{\partial}{\partial t}\mathbf{W}=\mathbf{P}\,(\mathrm{i});\ \frac{\partial}{\partial t}\mathbf{W}=-\frac{\partial}{\partial x}\mathbf{F}-\frac{\partial}{\partial y}\mathbf{G}(\mathrm{ii});\ \frac{\partial}{\partial t}\mathbf{W}=\mathbf{P}(\mathrm{iii}) \tag{9}$$

where the solution **W** in time t is used as an initial data for Equation (i), which is solved by $\mathscr{N}$-times repeated 2-stage Runge–Kutta method with time step $\Delta t/(2\mathscr{N})$, where $\Delta t/\mathscr{N}$

corresponds to the time scale of condensation and Δt comes from the stability condition of cell-vertex method for the equation (ii). The result from Equation (i) is then used as an initial data for Equation (ii), which is solved by the one step of cell-vertex method with the time step Δt. Finally the result from Equation (ii) is used as an initial data for Equation (iii), which is again solved by $\mathcal{N}$-times repeated Runge–Kutta method with time step $\Delta t/(2\mathcal{N})$. After this procedure we get the updated solution $\mathbf{W}$ in time $t + \Delta t$.

4. NUMERICAL RESULTS

Numerical results for two cases of an inviscid two-phase flow in Barschdoff nozzle [6] with the same inlet total pressure $p_{01} = 78390\,\text{Pa}$, two different inlet total temperatures and supersonic outlet velocity (no outlet boundary condition) are shown in Figure 2. Heat released by the nucleation slows down the supersonic flow resulting in a pressure jump called the condensation shock. The pressure distributions in Figure 2 show a well captured position of this pressure jump. The magnitude of pressure rise for $T_{01} = 373.15\,\text{K}$ (right graph in Figure 2) is slightly over-predicted most probably due to used inviscid flow model (higher jump is expectable without physical viscosity).

Second presented case is a viscous laminar flow in turbine cascade SE1050 [7–9]. Inlet angle is $\alpha_1 = 19.3°$, isentropic outlet Mach number $M_{2\text{is}} = 1.198$ and Reynolds number $Re = 1.5 \times 10^6$.

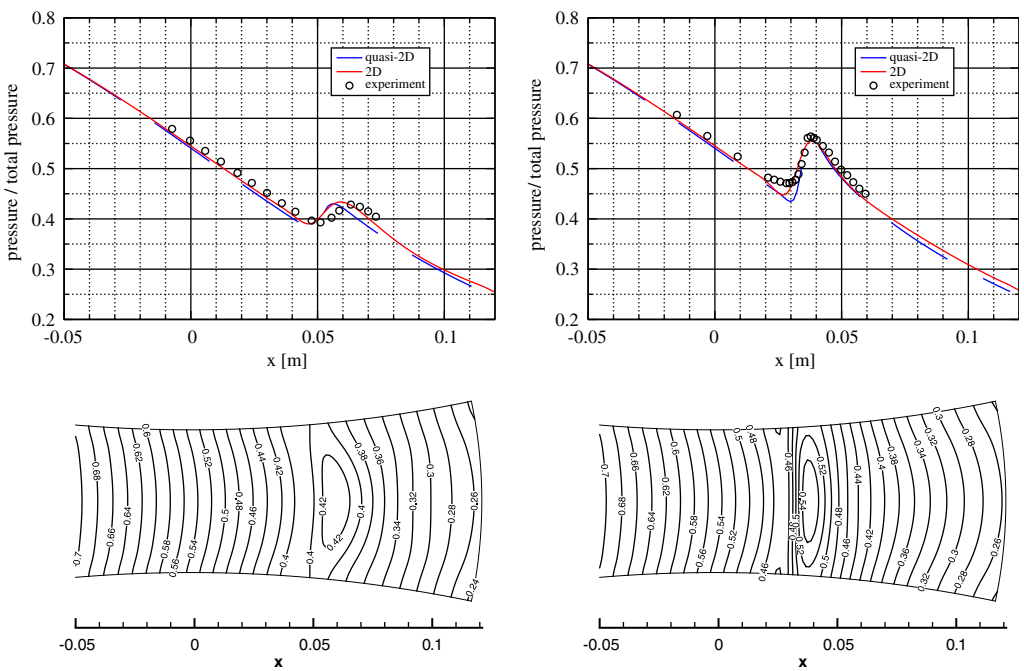

Figure 2. Pressure distribution along the nozzle axis (top) and experimental data. Isolines of p/p_0 ($\Delta p/p_0 = 0.02$) (bottom). $T_{01} = 380.50\,\text{K}$ (on the left), $T_{01} = 373.15\,\text{K}$ (on the right).

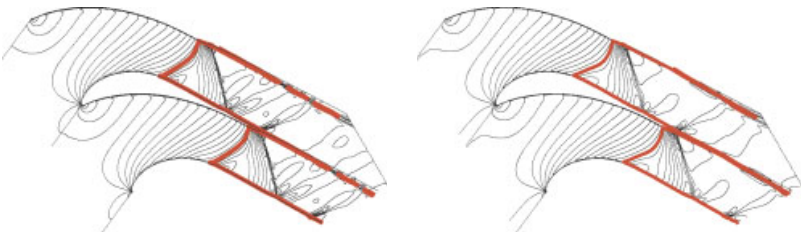

Figure 3. Mach number isolines $\Delta M = 0.05$. Left: Air $\gamma = 1.4$. Right: Steam *without* condensation, $\gamma = \gamma(T)$. Bold line denotes the sonic line.

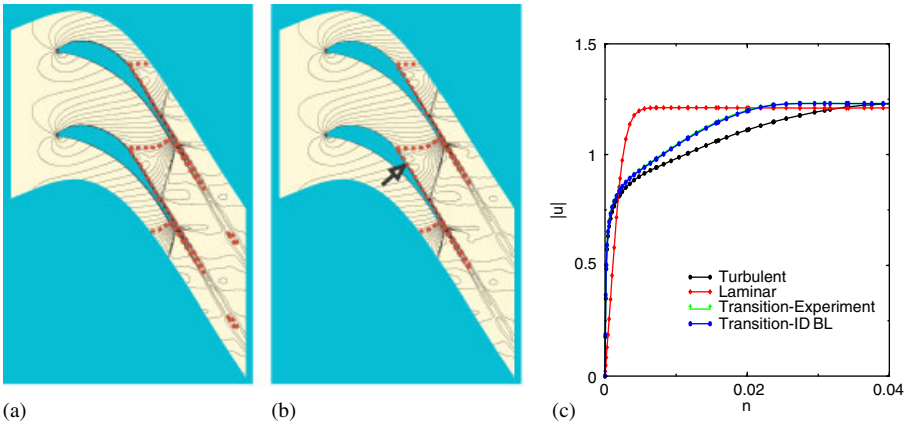

Figure 4. Flow in SE1050, explicit Roe (MUSCL) method, isolines of Mach number (marks denote the sonic line, $\Delta M = 0.05$). Velocity magnitude on suction side near the trailing edge. From left to right: (a) Fully turbulent flow model; (b) turbulent flow model with forced transition, arrow shows the transition onset; and (c) velocity magnitude in the normal direction (crossection on suction side near trailing edge). Turbulent computation starts from a laminar solution.

Mach number isolines in Figure 3 show the influence of the flowing media. The shock waves for the flow of steam ($\gamma = \gamma(T)$) are weaker than for the flow of air ($\gamma = 1.4$). The shape of the sonic line is also slightly different.

Turbulent flows of an ideal gas ($\gamma = 1.4$) in SE1050 obtained by cell-centred method is presented in Figure 4. Velocity distribution in the boundary layer on the suction side near the trailing edge is plotted in Figure 4(c). Substantial difference between laminar, turbulent computation and computation with transition can be observed, both in the velocity distribution across the boundary layer and in the slope of the graph in the vicinity of the blade affecting drag and hence losses. The convergence is measured by the loss coefficient fluctuations, because Barth's limiter causes the stall of the drop of the norm of the residual after a few order of magnitude.

5. CONCLUSIONS

Presented cell-vertex method shows a good agreement with experimental data for the two-phase inviscid flow with condensation in the nozzle. The local character of condensation model enables easy extension to 3D case. The implicit FV method (applied for the one-phase turbulent flow) with least square reconstruction and Barth's limiter [10] renders to be very efficient and allows to use CFL numbers in order of 200. Future investigation of turbulent flow with phase change is considered.

REFERENCES

1. Fořt J, Halama J. Numerical solution of transonic flow with condensation. *Proceedings of Conference Topical Problems of Fluid Mechanics 2004*, *IT CAS*, Prague, 2004, ISBN 80-85918-86-2, 47–50.
2. Hill PG. Condensation of water vapor during supersonic expansion in nozzles, part 3. *Journal of Fluid Mechanics* 1966; **3**:593–620.
3. Becker R, Döring W. Kinetische Behandlung der Keimbildung in übersättingten Dämpfen. *Annalen der Physik (Leipzig)* 1935; **24**(8):719–752.
4. Valha J. The flow of wet steam in through-flow part of steam turbine. *Doctoral Thesis*, SVUSS Běchovice, 1988, in Czech.
5. Šťastný M, Šejna M. Condensation effects in transonic flow through turbine cascade. *Proceedings of the 12th International Conference of the Properties of Water and Steam*. Begel House: New York, 1995; 711–719.
6. Barschdorff D. Verlauf der Zustandgrössen und gasdynamische Zuammenhänge der spontanen Kondensation reinen Wasserdampfes in Lavaldüsen. *Forschung Im Ingenieurwesen* 1971; **37**(5):146–157.
7. Šťastný M, Šafařík P. Experimental analysis data on the transonic flow past the plain turbine cascade. *Paper 90-GT-313*, ASME, 1990.
8. Fürst J, Janda M, Kozel K. Finite volume solution of 2D and 3D Euler and Navier–Stokes equations. In *Mathematical Fluid Mechanics*, Neustupa J, Penel P (eds). Birkhäuser: Basel, 2001; 173–194.
9. Louda P. Numerical solution of transonic turbulent flow through a turbine cascade. *Proceedings of Conference Topical Problems of Fluid Mechanics 2004*, *IT CAS*, Prague, 2004, ISBN 80-85918-86-2, 73–76.
10. Barth TJ. Aspects of unstructured grids and finite-volume solvers for the Euler and Navier–Stokes equations. *25th Computational Fluid Dynamics*, Von Karman Institute, 1994.

